Microsystem Technologies (2019) 25:4465–4474
https://doi.org/10.1007/s00542-019-04495-z

TECHNICAL PAPER

Design and fabrication of a D_{33}-mode piezoelectric micro-accelerometer

Ma-hui Xu[1,2] · Hui Zhou[1,3] · Lin-hui Zhu[1] · Jie-nan Shen[1,3] · Yi-bo Zeng[1] · Yong-jian Feng[2] · Hang Guo[1]

Received: 25 January 2019 / Accepted: 18 May 2019 / Published online: 29 June 2019
© Springer-Verlag GmbH Germany, part of Springer Nature 2019

Abstract

In this paper, a D_{33}-mode piezoelectric micro-accelerometer with $Pb_{1.1}(Zr_{0.52}Ti_{0.48})O_3$(PZT) thin film is designed, fabricated and tested. Both the polarization and deformation directions of the piezoelectric thin film are horizontal in this structure. With the high sensitivity and natural frequency, the D_{33}-mode piezoelectric micro-accelerometer possesses improved practicality. The influence of filling factor (Γ) and interdigital electrode width (b) on the output voltage is analyzed in this work. The micro-electro-mechanical systems technology is then used to fabricate the piezoelectric accelerometer device, which is based on the Sol–Gel PZT piezoelectric thin film. Performance of the piezoelectric accelerometer micro-devices with the different Γ and b is tested on the vibration table. The experimental results show that the sensitivity of D_{33}-mode piezoelectric accelerometer is inversely to the filling factor and interdigital electrode width. The piezoelectric accelerometer with a filling factor of 0.5 and an interdigital electrode width of 5 μm can generate an output voltage of 149.83 mV.

1 Introduction

The previous decades have witnessed rapid innovation in information technology. As the core of detection and measurement, sensors fabricated by the MEMS technology have gained applications in the fields of industrial inspection, wireless communication, aerospace and personal consumer electronics in recent years. Since the first miniature accelerometer came out in 1977, various MEMS-based accelerometers for detection have been proposed, including capacitive, piezoresistive, piezoelectric, tunnel current and resonant accelerometers (Chen et al. 1997; Sankar et al. 2012; Liu et al. 2014; Kubena et al. 1996; Zhao et al. 2016). Among them, piezoelectric accelerometers have captured many attentions due to their good dynamic performance, low power consumption and fast response (Iula et al. 1999; Noury 2002; Chang et al. 2010; Zhang et al. 2010).

In 1997, Devoe and Pisano (1997, 2001) developed an uniaxial micro-accelerometer with zinc oxide (ZnO) as the piezoelectric material for sensing. The sensitivity and resonant frequency of the accelerometer were measured to be 0.21 pC/g and 3.3 kHz, respectively. In 2002, Wang et al. (2002, 2003) developed a ring-shaped piezoelectric accelerometer. The accelerometer was based on a 5.6 μm PZT piezoelectric film prepared by the Sol–Gel approach. Compared with the ZnO piezoelectric film, the PZT piezoelectric film has higher piezoelectric coefficient. In addition, the piezoelectric coefficient is in proportion to the film thickness. Thus, thicker PZT film can effectively improve the sensitivity of the device. The sensitivity of their accelerometer ranged from 0.77 to 7.6 pC/g for different dimensions. In 2004, Zou et al. (2004, 2008) developed a highly symmetrical four-cantilever beam accelerometer, and each cantilever beam contained two piezoelectric film elements for sensing. This configuration can eliminate the film rupture caused by the expansion coefficient mismatch between the adjacent films. In addition, parallel connection of the bimorph films can also increase sensitivity of the device. This micro-accelerometer could detect the acceleration in the uniaxial (z-axis) and

✉ Hang Guo
hangguo@xmu.edu.cn

[1] Pen-Tung Sah Institution of Micro-Nano Science and Technology, Xiamen University, Xiamen 361005, China

[2] School of Aerospace Engineering, Xiamen University, Xiamen 361005, China

[3] School of Physical Science and Technology, Xiamen University, Xiamen 361005, China

the triaxial (x-axis, y-axis and z-axis) directions. However, the sensitivity was relatively low. Sensitivity of x-, y- and z-axis was 0.39, 1.13, and 0.88 mV/g, respectively. In 2011, Shanmugavel et al. (2011) developed a micro-accelerometer with interdigital electrodes deposited on the cantilever beam using low-resistance silicon and silicon-on-insulator (SOI), respectively. This accelerometer showed good output performance and a wide working frequency. However, the specific value of sensitivity was not mentioned in their work, which is a critical parameter to evaluate the performance of an accelerometer. In 2014, Donghwan et al. (Kim et al. 2014) developed a micro-accelerometer. The device was comprised of a bulk-silicon cylinder at the center that was connected to six silicon cantilevers on which the piezoelectric thin film materials and interdigital electrodes were deposited. The filling factor of the interdigital electrode is the main geometrical parameter to influence the signal to noise ratio of the micro-device. Although many MEMS-based piezoelectric accelerometers have been studied, there are still many improvements need to be done in terms of the device structure, sensitivity, piezoelectric film, and piezoelectric property measurement. The cantilever structure in most of piezoelectric micro-accelerometer is a "sandwich" where the bottom electrode, piezoelectric material, top electrode are deposited on the cantilever beam one by one. When acceleration is applied, movement of the seismic mass will induce an extensive or compressive deformation of the cantilever beam in the horizontal direction. Surface charge is generated on both top and bottom of the piezoelectric material that are deposited on the cantilever beam. However, the sensitivity in the horizontal direction of the D_{31}-mode piezoelectric accelerometers is generally not satisfactory due to the limited deformation in the horizontal direction. To improve the sensitivity in the horizontal direction, a piezoelectric accelerometer structure based on the D_{33}-mode is introduced in this work. Both the polarization and deformation of the piezoelectric thin film are in the horizontal direction. In addition, the longitudinal piezoelectric coefficient d_{33} of the PZT material is much higher than its transverse piezoelectric coefficient d_{31}, decreasing the requirement on the thickness of the piezoelectric materials in fabrication of the micro-accelerometer. For the same thickness of the piezoelectric materials, the D_{33}-mode accelerometer can output a stronger voltage signal than the D_{31}-mode accelerometer. Thus, the D_{33}-mode could improve the sensitivity of the piezoelectric micro-accelerometer with the unaffected natural frequency, increasing the practicality of piezoelectric micro-accelerometers.

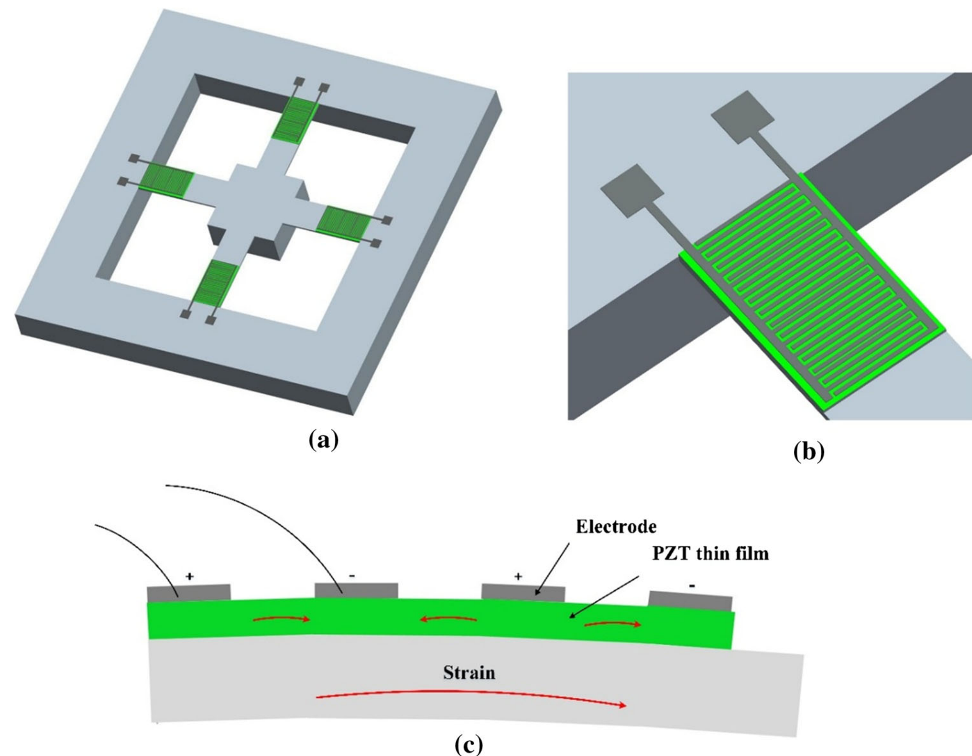

Fig. 1 Structure of the D_{33}-mode piezoelectric accelerometer. **a** 3D structure of the D_{33}-mode piezoelectric accelerometer. **b** The interdigital electrode structure of the D_{33}-mode piezoelectric accelerometer. **c** The polarization and deformation directions of the piezoelectric thin film

2 Device design and finite element method simulation

The D_{33}-mode piezoelectric accelerometer consists of one seismic mass and four suspended cantilever beams on which the four piezoelectric thin film sensing elements are deposited. Both the polarization and deformation directions of the piezoelectric thin film are horizontal, as shown in Fig. 1c. Upon an acceleration or inertial force, the seismic mass will move along the vertical direction, leading to a horizontal direction deformation of cantilever beam and PZT thin film. Certain amount of bounded charges is generated on the piezoelectric thin film due to the piezoelectric effect, and the bounded charge is collected with the interdigital electrodes. The sensitivity of accelerometer can be obtained in terms of the output voltage signals.

Table 1 Structural parameters of the D_{33}-mode piezoelectric micro-accelerometer

Parameter	Value
Length of seismic mass (μm)	2000
Width of seismic mass (μm)	2000
Thickness of seismic mass (μm)	450
Length of cantilever beam (μm)	2500
Width of cantilever beam (μm)	1300
Thickness of cantilever beam (μm)	4.5
Length of PZT thin film (μm)	1250
Width of PZT thin film (μm)	1300
Thickness of PZT thin film (μm)	1.3

Theoretical analysis is done to predict the sensitivity and natural frequency of the D_{33}-mode piezoelectric accelerometer. The whole structure of the D_{33}-mode can be regarded as composed of many interdigital electrodes in parallel. To simplify the analysis, the filling factor Γ is used to represent the volume ratio of the effective piezoelectric part to the whole element in a cell, i.e. Γ is expressed as the ratio of the distance between two adjacent interdigital electrodes and the distance between the centers of two adjacent interdigital electrodes, which is,

$$\Gamma = \frac{d}{d+b}, \tag{1}$$

where d is the width between two adjacent interdigital electrodes, and b is the width of a single interdigital electrode.

The charge generated due to the deformation of the piezoelectric material can be derived as,

$$Q = \Gamma \cdot \int_0^{0.5l} D_3 w dx = \frac{\Gamma}{32} d_{33} w \frac{E_p}{EI_{ep}} \left(a + \frac{h_{PZT}}{2}\right) m_0 g a l^2, \tag{2}$$

where E_p is the Young's modulus of the PZT thin film, h_{PZT} is its thickness, w and l are the thickness and length of the cantilever beam, respectively, and m_0 and g are the mass of the seismic mass and the gravitational acceleration, respectively.

The capacitance can be expressed as,

$$C = \varepsilon_0 \varepsilon_{33} \frac{h \cdot w}{d} \cdot \frac{0.5l}{d+b}, \tag{3}$$

where ε_{33} is the effective dielectric constant of the piezoelectric material, and ε_0 is the vacuum permittivity.

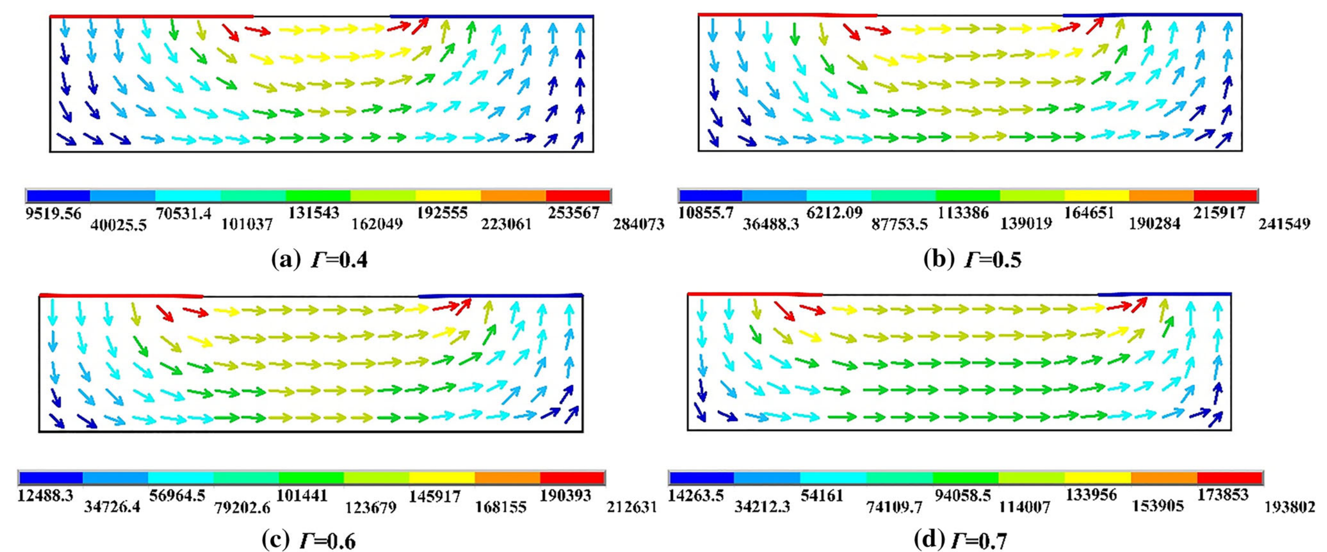

Fig. 2 Polarization electric field distribution in the piezoelectric thin film at different Γ

According to the relationship between the voltage and charge for the piezoelectric material, the sensitivity of the D_{33}-mode piezoelectric micro-accelerometer can be derived as,

$$S_{vz} = \frac{Q}{C \cdot a_z} = \frac{\frac{\Gamma}{32} d_{33} w \frac{E_p}{EI_{ep}} \left(a + \frac{h_{PZT}}{2}\right) m_0 g a l^2}{\varepsilon_0 \varepsilon_{33} \frac{h \cdot w}{d} \cdot \frac{05l}{d+b} \cdot a_z}. \tag{4}$$

In the dynamic analysis, the cantilever beam is regarded as a mass spring system and the lowest resonant frequency of the D_{33}-mode piezoelectric micro-accelerometer is obtained through a Rayleigh–Ritz method (Kampen and Wolffenbuttel 1998; Kollias and Avaritsiotis 2005). The natural frequency can be derived as,

$$f = \omega/2\pi = \frac{1}{4\pi}\sqrt{\frac{\frac{1}{EIeq} + \frac{1}{EI}}{\left[\frac{11}{560}\rho w (h + h_{PZT}) \cdot \frac{l^4}{(EI_{eq})^2} + \frac{383}{1680}\rho w h \cdot \frac{l^4}{(EI)^2} + \frac{1}{6} m \cdot \frac{l^3}{(EI)^2}\right]}}. \tag{5}$$

Detailed calculation of voltage sensitivity and natural frequency of D_{33}-mode piezoelectric micro-accelerometer can be found in our previous work (Zhou et al. 2016). The structural parameters of the D_{33}-mode piezoelectric micro-accelerometer are shown in Table 1.

In the analysis of D_{33}-mode piezoelectric micro-accelerometer, the piezoelectric performance and polarization of the electrode are mainly influenced by the filling factor Γ and interdigital electrode width b. Finite element analysis (FEA) in ANSYS is used to analyze the distribution of the polarization electric field in the piezoelectric thin film at different Γ and different b, as shown in Figs. 2 and 3, respectively.

As shown in Fig. 2, the polarization electrical field tends to decrease as the Γ gradually increases. In fact, the increasing Γ will gradually increase the distance between adjacent interdigital electrodes, but the increased interspace between adjacent interdigital electrodes will weaken the electric field that will lead to the low polarization electric field in the PZT thin film. Based on these, a lower value of Γ can enhance the intensity of polarization electric field and improve the piezoelectric effect of the piezoelectric thin film. In addition, upon the filling factor is constant, the polarization electric field in the piezoelectric thin film is found to increase with the gradual reduction of the b value, as shown in Fig. 3. Therefore, the device performance can be improved by decreasing the value of b under the premise of satisfying the lithographic exposure accuracy of the microfabrication process.

Figures 4 and 5 show the voltage distribution and natural frequency of the piezoelectric accelerometer with the values of Γ of 0.5 and b of 5 μm, respectively. The sensitivity of the D_{33}-mode piezoelectric micro-accelerometer in terms of voltage can be obtained with the integral of the voltage in the entire electrode region. Values of parameters in FEA in ANSYS for numerical simulation are shown in Table 2. The PZT thin film is divided into several parts in order to improve the accuracy of the analysis. Mechanical–electrical coupling for calculating the piezoelectric effect is added to the left and right sides of the partitioned PZT thin films. Acceleration or force is loaded to the seismic mass in

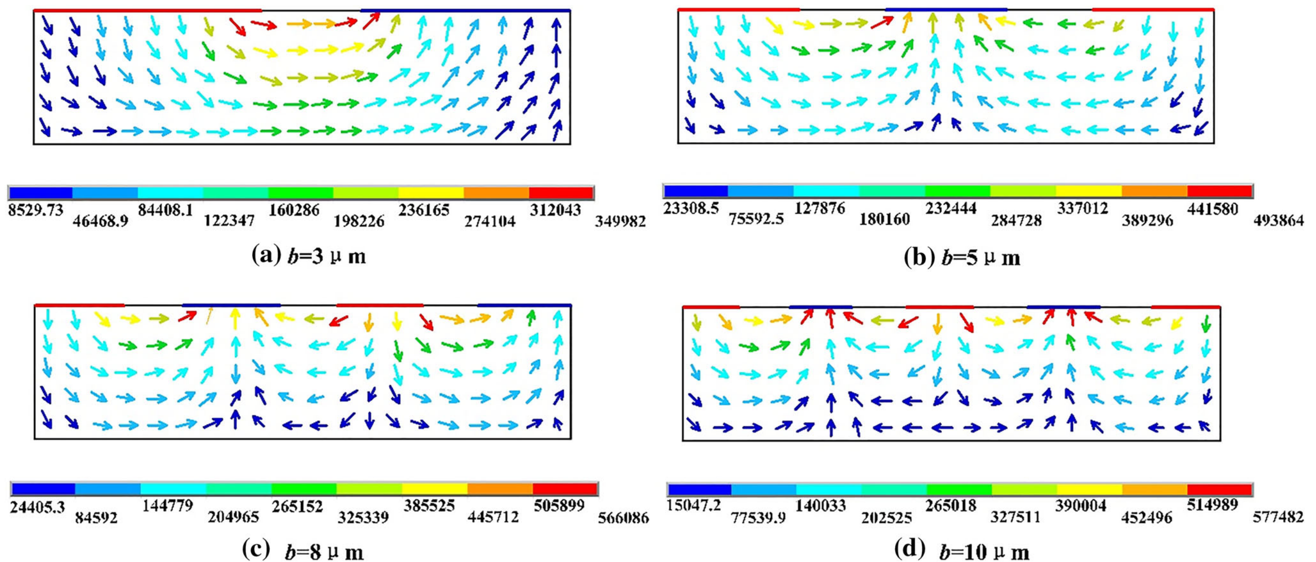

Fig. 3 Polarization electric field distribution in the piezoelectric thin film at different b

the vertical direction (z-direction), and constraints are applied to the external frame.

When a vertical acceleration is loaded to the piezoelectric accelerometer, a stress in the horizontal direction occurs in piezoelectric thin films. The maximum voltage of 151.52 mV is generated in the electrodes, and the natural frequency of the fundamental mode is 3048.8 Hz, demonstrating that the presented D_{33}-mode piezoelectric micro-accelerometer can work in a wide frequency range. Also, the natural frequency of the fundamental mode is usually higher than the external excitation frequencies and differs from frequencies of the other higher-order modes. This feature of the piezoelectric micro-accelerometer can avoid the interference from external signals and accurately output the voltage signal.

Furthermore, the results of the modal analysis are verified by the structural response to the applied excitation under different frequencies by using the harmonic response analysis, as shown in Fig. 6. An impulse of output response of the device is observed when the scanning frequency reaches to 3084.83 Hz. This can be attributed to the resonance between the loading frequency and the natural frequency of the structure. Thus, the natural frequency in modal analysis agrees well with that of harmonic response analysis.

3 Fabrication

The micro-device of the PZT-based D_{33}-mode piezoelectric accelerometer is fabricated by using the MEMS technology. A 4-in. (100) n-type silicon wafer with thickness of 450 μm is used as substrate. The fabrication is followed by growth of silica (SiO_2) layers, spin coating of PZT thin film, deposition of Pt/Ti electrode and deep reactive ion etching (DRIE) of silicon. Figure 7 shows the microfabrication process flow. In the first step, the Si wafer is transferred to a tube furnace and oxidized at 1100 °C for 2 h, and a 200 nm SiO_2 layer is grown on both sides of the Si wafer. The SiO_2 layer can avoid direct contact between the Ti layer and the Si substrate (Fig. 7a). Then the wafer is patterned and etched to obtain the cantilever beam. The SiO_2 layer at the through-hole is removed by using the buffered oxide etch (BOE), and then the exposed silicon is etched to 4.5 μm by using plasma etching. Thus, the cantilever beam structure is obtained (Fig. 7b). A Ti layer with a thickness of 5 nm is sputtered on the SiO_2 surface to increase adhesion between the SiO_2 layer and the PZT thin film (Fig. 7c). The PZT solution is deposited on the wafer by spin-coating at 2500 rpm for 30 s. After deposition, each layer is subjected to a two-step pyrolysis sequence. A 1-min heat treatment at 300 °C is immediately followed by an annealing at 600 °C for 30 min in a vacuum tube to make the PZT layer to be crystallized. A multi-step spin-coating is employed to achieve the desired film thickness (1.3 μm). The PZT thin film is patterned with lithography and then etched (Fig. 7d). Top electrode is obtained by the reverse lithography with positive photoresist, together with sputtering, stripping and subsequent annealing process. In order to further improve the sensitivity of piezoelectric micro-accelerometer, the piezoelectric thin film needs to be polarized after the annealing of the top electrode. The polarization voltage is about 2–3 times that of the coercive field strength and the polarization time is 15 min (Fig. 7e). A 3 μm SiO_2 layer and a 13 μm photoresist layer (AZ4620) are coated on the backside of the Si wafer one by one by using the PECVD technology and spin-coating,

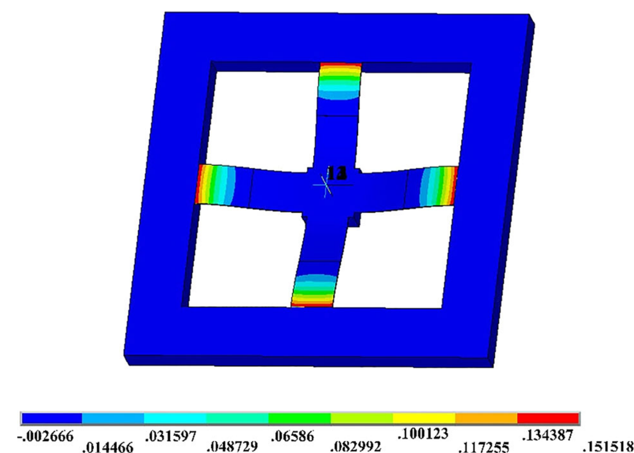

Fig. 4 Voltage distribution in the D_{33}-mode piezoelectric micro-accelerometer

Table 2 Values of parameters used in the ANSYS for numerical simulation

Material	Si	PZT
E (Pa)	1.29×10^{11}	–
σ	0.18	–
ρ (kg/m^3)	2330	7550
ε_{11} (F/m)	–	1.5×10^{-9}
ε_{33} (F/m)	–	1.2×10^{-8}
C_{11} (N/m^3)	–	1.6×10^{-11}
C_{12} (N/m^3)	–	-5.3×10^{-12}
C_{13} (N/m^3)	–	7.2×10^{-12}
C_{33} (N/m^3)	–	2.3×10^{-11}
C_{44} (N/m^3)	–	6.0×10^{-11}
C_{66} (N/m^3)	–	4.3×10^{-11}
d_{15} (C/N)	–	1.5×10^{-10}
d_{31} (C/N)	–	3.0×10^{-11}
d_{33}(C/N)	–	8.5×10^{-11}

Fig. 5 Mode analysis of the D_{33}-mode piezoelectric micro-accelerometer **a** The 1st mode (*f* = 3048.83 Hz). **b** The 2nd mode (*f* = 9511.86 Hz). **c** The 3rd mode (*f* = 9531.53 Hz). **d** The 4th mode (*f* = 36315.3 Hz)

respectively. The SiO_2 layer and photoresist layer can be used as the mask layer to protect the seismic mass (Fig. 7f). The SiO_2 layer is patterned and etched to expose the Si substrate (Fig. 7g), and then deep reactive ion etching is used to thinned the silicon. The silicon wafer is adhered to a 7740 glass by using paraffin wax and then the silicon wafer is etched from backside. The etching should be closely monitored to avoid the damage of cantilever beam. After a 107-min DRIE treatment, a 445.5 μm through-holes can be obtained (Fig. 7h). Figure 8 shows the typical SEM images of the developed PZT thin film. The laser scanning confocal microscopy graph of the D_{33}-mode piezoelectric accelerometer is shown in Fig. 9.

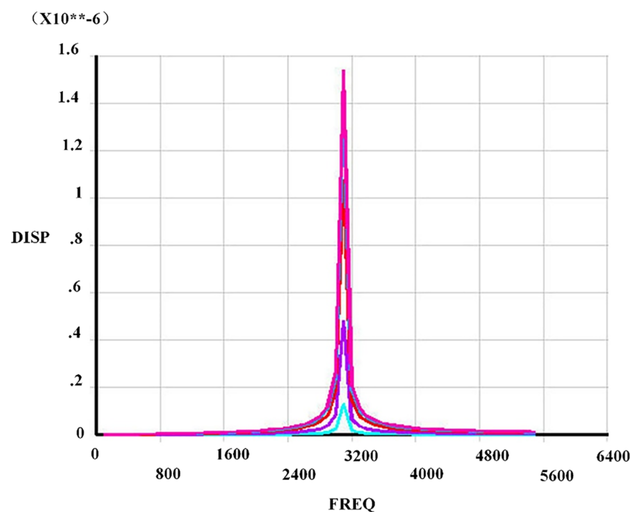

Fig. 6 Curves of harmonic response analysis using FEA in ANSYS for the D33-mode piezoelectric micro-accelerometer

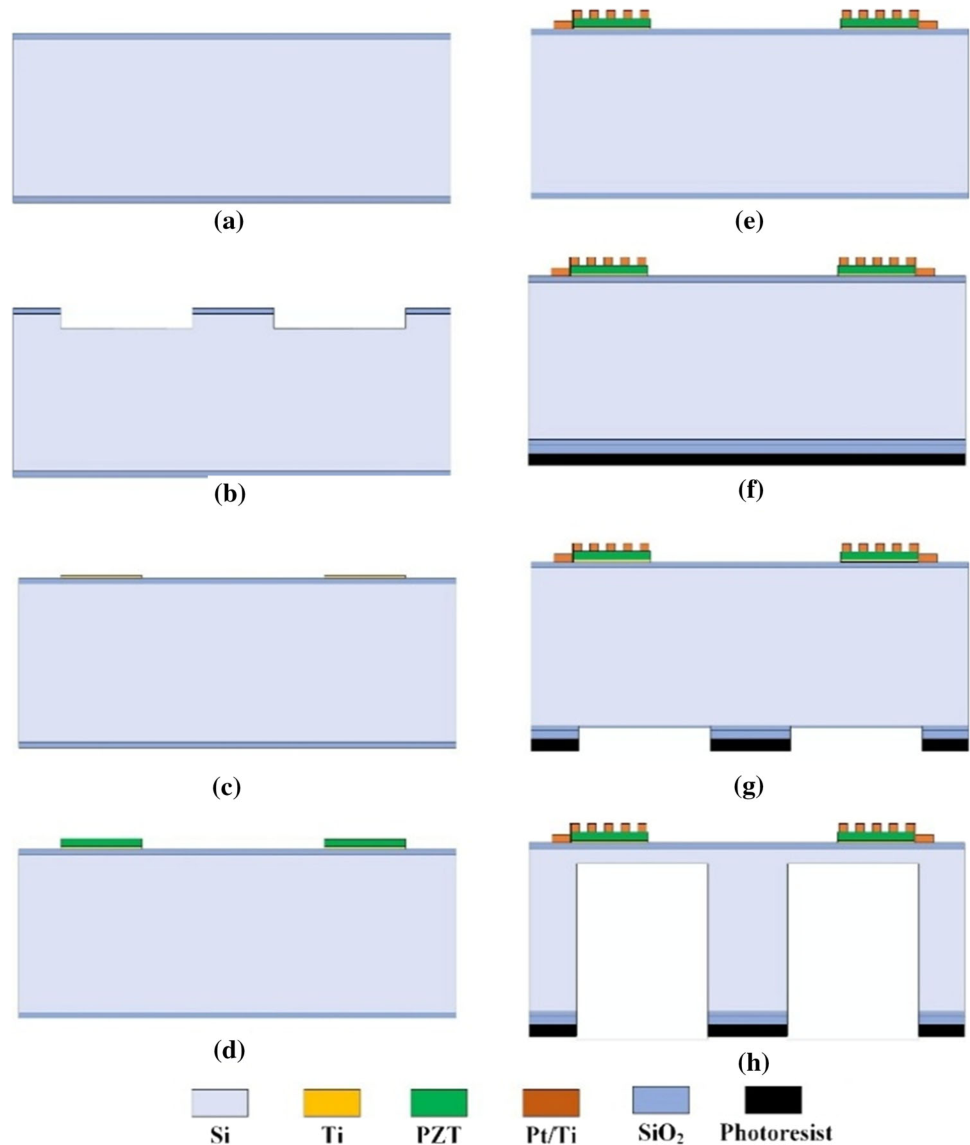

Fig. 7 Fabrication process of the D_{33}-mode piezoelectric accelerometer. **a** Growth of SiO_2 layer by thermal oxidation. **b** Patterned and etched to obtain the cantilever beam. **c** Deposition of Ti layer. **d** Preparation of PZT thin film. **e** Deposition of Pt/Ti layer for top electrode. **f** Growth of SiO_2 layer on the back side of the silicon wafer by PECVD. **g** SiO_2 at through-hole was etched by BOE. **h** Release of the seismic mass structure

4 Measurement

The sensitivity characterization is performed to evaluate the performance of the piezoelectric micro-accelerometer. The measurement circuit in the vertical direction (*z*-direction) is laid on the circuit board. The micro-device is connected to the soldering point on the ceramic circuit board to perform the signal output. Test circuit is designed as a sandwich structure. The micro device of the piezoelectric accelerometer and the test circuit are distributed at the bottom of the sandwich structure. During the test, the piezoelectric accelerometer is connected to two charge amplifiers, one of which converts the charge signal into the voltage signal, and the other one is a voltage amplifier. The amplifier delivers a feedback capacitance of 10 pF and an amplification of 500 mV/pC. The top circuit board could be used as a low-pass filter to reduce the noise generated in the circuit. Package of the D_{33}-mode piezoelectric accelerometer package is shown in Fig. 10. The piezoelectric micro-accelerometer is connected to an impact table for test. Power generated from the collision with anvil is converted into an impulsive load onto the piezoelectric micro-accelerometer, resulting in a charge signal. The charge signal is converted to a voltage signal by the charge amplifier, and performance of the piezoelectric accelerometer could be evaluated based on the maximum output voltage. The test device setup for the D_{33}-mode

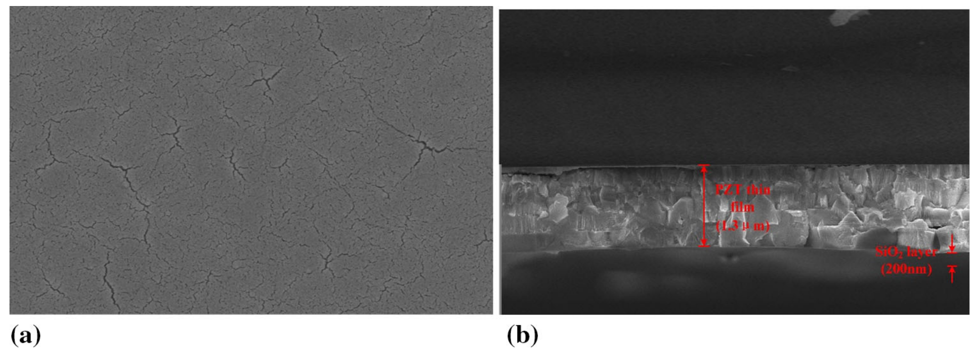

Fig. 8 SEM images of the PZT thin film. **a** The surface morphology of the PZT thin film. **b** The cross-sectional of the PZT thin film

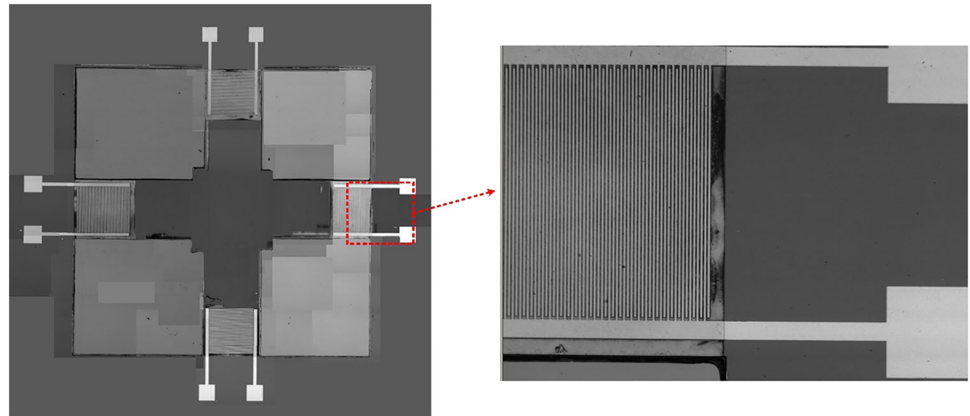

Fig. 9 The laser scanning confocal microscopy graph of the D_{33}-mode piezoelectric accelerometer

piezoelectric micro-accelerometer in this work is shown in Fig. 11.

5 Results and discussion

Acceleration applied to the D_{33}-mode piezoelectric micro-accelerometer could be changed by adjusting the height of the dropping hammer. To investigate the effect of Γ and b on the output voltage, various accelerations in vertical direction (z-direction) are applied to the piezoelectric accelerometer with different values of Γ and b, as shown in Fig. 12a, b, respectively.

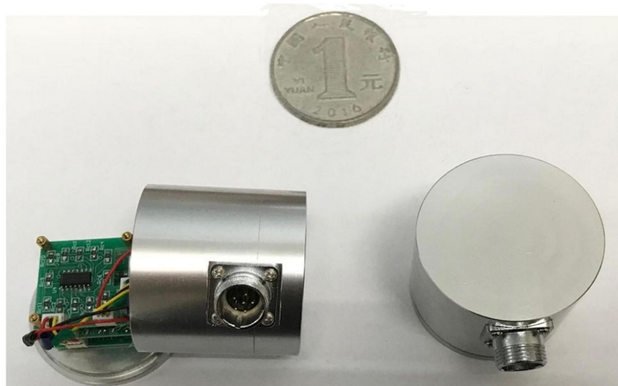

Fig. 10 The D_{33}-mode piezoelectric accelerometer after packaged

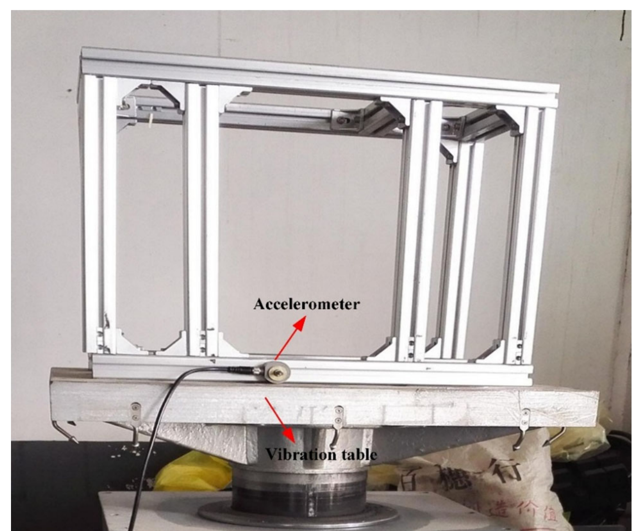

Fig. 11 The test device for the D_{33}-mode piezoelectric accelerometer

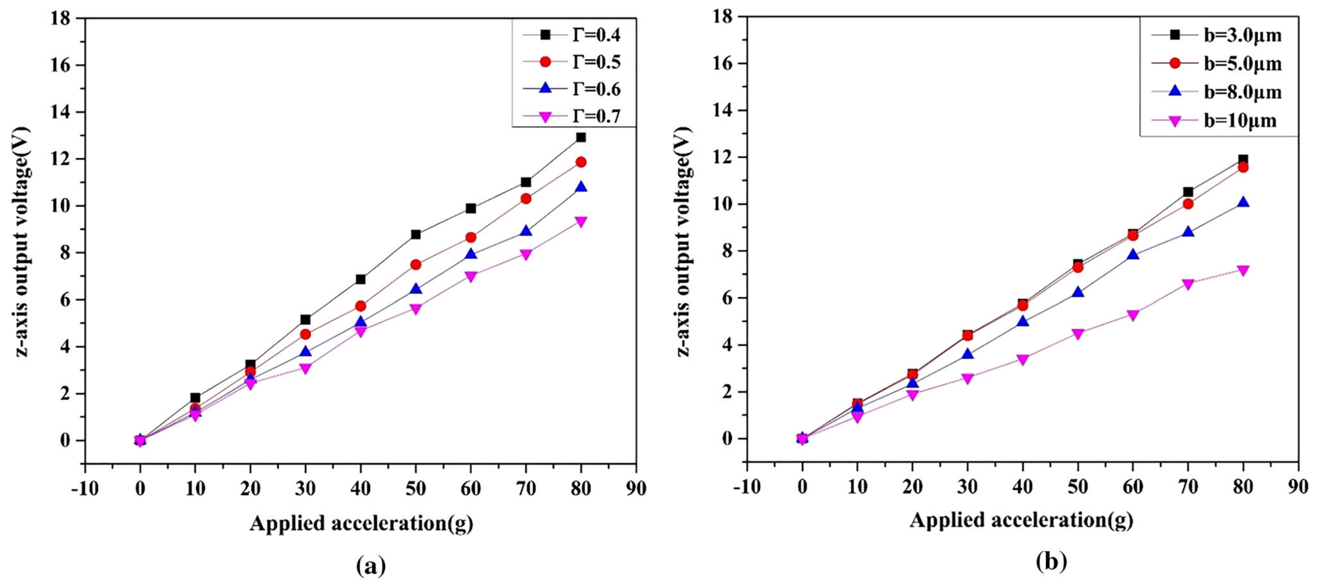

Fig. 12 Test results of the D_{33}-mode piezoelectric accelerometer. **a** The effect of different Γ on the accelerometer output voltage. **b** The effect of different b on the accelerometer output voltage

It can be seen from Fig. 12 that the parameters of Γ and b play important roles to the output voltage signal of the D_{33}-mode piezoelectric micro-accelerometer. Under the same acceleration in the vertical direction (z-direction), the output voltage gradually decreases as the Γ increase, while the voltage signal increases as the b decreases. With the values of Γ of 0.5 and b of 5 μm and an acceleration of 1 g applied in the vertical direction (z-direction), the piezoelectric accelerometer delivers a voltage of 149.83 mV output from the interface circuit. This result shows that the developed D_{33}-mode piezoelectric micro-accelerometer in this work can be practically used in engineering.

6 Conclusions

In this paper, a D_{33}-mode piezoelectric accelerometer based on the PZT thin film is developed. Compared with the D_{31}-mode piezoelectric micro-accelerometer, its polarization and deformation of the piezoelectric thin film are in the horizontal direction. The intrinsic frequency is almost unaffected while the sensitivity can be greatly improved. MEMS technology is used to fabricate the D_{33}-mode piezoelectric micro-accelerometer, especially, the Sol–Gel method is used for deposition of the PZT thin films. Performance of the piezoelectric micro-accelerometer is tested and results show that smaller filling factor and narrower electrode interspace are beneficial for a high voltage output. In the future, the designed structure and processing technology will be further improved and optimized to meet requirements in different application areas, including aerospace activating vehicle safety systems, industrial monitoring of machine and vibration, and biomedical inspections.

Acknowledgements This work is financially supported by the Scientific Research and Development Program of City of Xiamen (3502Z20143003) and the Fujian Province Collaboration Program between Industry and University (2015H6021).

References

Chang C, Tran H, Wang J, Fuh K, Lin L (2010) Direct-write piezoelectric polymeric nanogenerator with high energy conversion efficiency. Nano Lett 10(2):726–731

Chen H, Shen S, Bao M (1997) Over-range capacity of a piezoresistive microaccelerometer. Sens Actuators A 58(3):197–201

Devoe DL, Pisano AP (1997) A fully surface-micromachined piezoelectric accelerometer. Solid State Sens Actuators 2:1205–1208

Devoe DL, Pisano AP (2001) Surface micromachined piezoelectric accelerometers (PiXLs). J Microelectromechanical Syst 10(2):180–186

Iula A, Lamberti N, Pappalardo M (1999) Analysis and experimental evaluation of a new planar piezoelectric accelerometer. IEEE/ASME Trans Mechatron 4(2):207–212

Kampen R, Wolffenbuttel R (1998) Modeling the mechanical behavior of bulk-micromachined silicon accelerometers. Sens Actuators A 64(2):137–150

Kim D, Hewa-Kasakarage NN, Hall NA (2014) A theoretical and experimental comparison of 3-3 and 3-1 mode piezoelectric microelectromechanical systems (MEMS). Sens Actuators A 219:112–122

Kollias A, Avaritsiotis J (2005) A study on the performance of bending mode piezoelectric accelerometers. Sens Actuators A 121(2):434–442

Kubena RL, Atkinson GM, Robinson WP, Stratton FP (1996) A new miniaturized surface micromachined tunneling accelerometer. IEEE Electron Device Lett 17(6):306–308

Liu Y, Zhao YL, Tian B, Sun L, Yu ZY, Jiang ZD (2014) Analysis and design for piezoresistive accelerometer geometry considering sensitivity, resonant frequency and cross-axis sensitivity. Microsyst Technol 20:463–470

Noury N (2002) A smart sensor for the remote follow up of activity and fall detection of the elderly. In: 2nd annual international IEEE-EMB special topic conference on microtechnologies in medicine & biology, pp 314-317

Sankar AR, Jency JG, Das S (2012) Design, fabrication and testing of a high performance silicon piezoresistive Z-axis accelerometer with proof mass-edge-aligned-flexures. Microsyst Technol 18:9–23

Shanmugavel S, Yao K, Luong TD, Oh SR, Chen YF, Tan CY, Gaunekar A, Ng PH, Li MH (2011) Miniaturized acceleration sensors with in-plane polarized piezoelectric thin films produced by micromachining. IEEE Ultrason Ferroelectr Freq Control Soc 58(11):2289–2296

Wang L, Deng K, Zou L, Wolf RA, Davis RJ, Trolier-McKinstry S (2002) Microelectromechanical systems (MEMS) accelerometers using lead zirconate titanate thick films. IEEE Electron Dev Lett 23(4):182–184

Wang LP, Wolf RA, Wang Y, Deng K, Zou L, Davis RJ, Trolier-McKinstry S (2003) Design, fabrication, and measurement of high-sensitivity piezoelectric microelectromechanical systems accelerometers. J Microelectromechanical Syst 12(4):433–439

Zhang S, Jiang X, Lapsley M, Moses P, Shrout T (2010) Piezoelectric accelerometers for ultrahigh temperature application. Appl Phys Lett 96(1):1–3

Zhao L, Dai B, Yang B, Liu XJ (2016) Design and simulations of a new biaxial silicon resonant micro-accelerometer. Microsyst Technol 22:2829–2834

Zhou H, Han R, Xu M, Guo H (2016) Study of piezoelectric accelerometer based on D_{33} mode. In: Proceedings of the 2016 IEEE symposium on piezoelectricity, acoustic waves and device applications, pp 61–65

Zou Q, Tan W, Kim ES, Loeb GE (2004) Highly symmetric tri-axis piezoelectric bimorph accelerometer. In: 17th IEEE international conference on micro electro mechanical systems, pp 197–200

Zou Q, Tan W, Kim ES, Loeb GE (2008) Single- and tri-axis piezoelectric-bimorph accelerometers. J Microelectromechanical Syst 17:45–57

Publisher's Note Springer Nature remains neutral with regard to jurisdictional claims in published maps and institutional affiliations.